Available online at www.sciencedirect.com
SCIENCE DIRECT®
International Journal of Solids and Structures 42 (2005) 255–269
INTERNATIONAL JOURNAL OF SOLIDS and STRUCTURES
www.elsevier.com/locate/ijsolstr

Buckling load of seismic isolators affected by flexibility of reinforcement

Hsiang-Chuan Tsai [a,*], James M. Kelly [b]

[a] Department of Construction Engineering, National Taiwan University of Science and Technology, P.O. Box 90-130, Taipei 106, Taiwan
[b] Pacific Earthquake Engineering Research Center, University of California, Berkeley, USA

Received 22 September 2003; received in revised form 20 July 2004
Available online 15 September 2004

Abstract

Using the thinner steel reinforcing plates in the elastomeric multilayer isolators could reduce the weight of the isolators but would have a large effect on the buckling load of an isolator, which cannot be analyzed by the Haringx theory, a traditional approach on the stability analysis of rubber bearings. The buckling load of the isolators, which includes the effect of the flexibility of the steel reinforcing plates, is analyzed by a beam theory in which shear deformation and warping of the cross-section are considered. Pressure distributions in the elastomeric layer bonded to flexible reinforcements under compression force, bending moment and warping moment are derived from an assumed displacement field, from which the warping-related parameters used in the beam theory are established. The thickness of the steel reinforcement in the isolators is determined from the buckling load of the isolators, which is solved from a cubic equation established by the beam theory.

Keywords: Base isolation; Elastomeric bearing; Buckling load

1. Introduction

A laminated rubber bearing used in seismic isolation has many layers of elastomer reinforced by steel plates. The reinforcing plates constrain the elastomer from lateral expansion and provide a high compression and bending stiffness, but have no effect on the shear stiffness. To analyze the compression stiffness and bending stiffness of the isolators, the steel reinforcement is treated as completely rigid; the elastomeric layer is assumed as completely buck-incompressible (Gent and Lindley, 1959; Gent and Meinecke, 1970). Kelly

* Corresponding author. Tel.: +8862 27376581; fax: +8862 27376606.
E-mail address: hctsai@mail.ntust.edu.tw (H.-C. Tsai).

0020-7683/$ - see front matter © 2004 Elsevier Ltd. All rights reserved.
doi:10.1016/j.ijsolstr.2004.07.020

(1997) presents a "pressure approach" to obtain the major terms of the compression stiffness and bending stiffness of an incompressible elastic layer bonded to rigid plates. The "pressure approach" is then extended to analyze the compression stiffness and bending stiffness of the fiber-reinforced isolators where the reinforcement is treated as extensible (Tsai and Kelly, 2001, 2002a,b). When deriving the stiffness of bonded elastic layers, the deformation of the elastic layer is always assumed that horizontal planes remain plane and vertical lines become parabolic. The derived stiffness based on these two assumptions has been shown to close to the results of finite element analysis (Tsai and Lee, 1998, 1999).

The isolators, whose deformation is dominated by shear, are always used to carry vertical load. It is essential that their stability can be assessed in a reasonable simple manner. Haringx theory (1948), which includes the shear effect in the stability analysis of the elastic column, becomes the standard approach to analyze the stability of multilayer elastomeric bearings (Gent, 1964), and is extended to the viscoelastic column to study the behavior of energy dissipation in the isolators (Tsai and Hsueh, 2001). In Haringx theory, plane sections that are normal to the beam axis before deformation remain plane but not necessarily normal after deformation. In other words, applying Haringx theory to analyze the buckling behavior of elastomeric isolators is based on the premise that the steel reinforcing plates are rigid in bending. A beam theory has been developed that extends Haringx theory by allowing the cross-sections to distort into a non-planar surface (Kelly, 1994; Tsai and Kelly, in press).

For the design purpose, the thickness of the reinforcing plates is selected by rule of thumb since there is no information as to how thick the plates need to be to ensure that they are rigid. To reduce the weight of the isolators, it would be advantageous to use thinner steel plates. This modification would have a large effect on the buckling load of an isolator. To understand the influence of the flexibility of the reinforcing plates on the buckling of the isolators, a theoretical approach on the stability analysis of isolators is developed in this paper. The isolator is idealized in a plane-strain state. Pressure distributions in the elastomeric layer bonded to flexible reinforcements under compression force, bending moment and warping moment are derived, which are utilized to determine the effective stiffness and the warping function of the cross-section. After the warping-related parameters are established, the beam theory of Tsai and Kelly (in press) is applied to study the buckling load of the isolators. Since the beam theory of Tsai and Kelly utilizes the linear stiffness, the infinitesimal deformation theory is employed in the elastomeric layers and reinforcements to derive the effective stiffness of seismic isolators.

2. Pressure distribution in elastomeric layers

To analyze the stiffness of the isolator, a single layer of elastomer bonded between reinforcing plates is considered. The shape of the isolator is idealized as an infinite-long rectangular strip. As shown in Fig. 1, the elastomeric layer has a width of $2a$ and a thickness of t_e. Its top and bottom surfaces are perfectly bonded to reinforcements that have a thickness of t_f. A coordinate system (x, y, z) is established by locating the origin at the center of the elastomeric layer and the y coordinate direction is attached to the infinitely

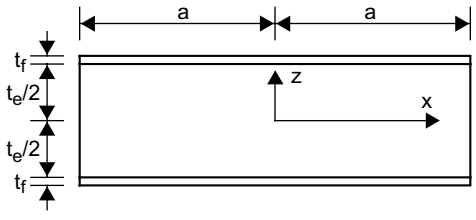

Fig. 1. Single layer of elastomer bonded to reinforcements.

long side. The deformation of the pad is in a plane strain state, so that the displacement component in the y direction vanishes.

Under a compressive force P in the vertical direction, the thickness of the elastomeric layer is reduced by Δ as shown in Fig. 2. When subjected to a bending moment M, the top and bottom reinforcements remain plane and rotate to form an angle ψ as shown in Fig. 3. Under a warping moment Q as shown in Fig. 4, the deformation of the reinforcements is measured by $\phi\Omega(x)$ where Ω is a function describing the warping shape and ϕ is the multiplier of the warping shape. The warping function is a cubic function defined as

$$\Omega(x) = \left(\frac{x}{a}\right)^3 + \omega\left(\frac{x}{a}\right) \tag{1}$$

where ω is the warping coefficient to be determined.

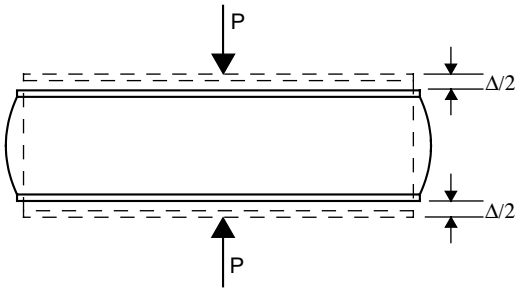

Fig. 2. Deformation under compression force.

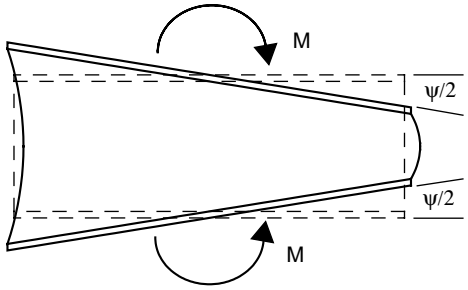

Fig. 3. Deformation under bending moment.

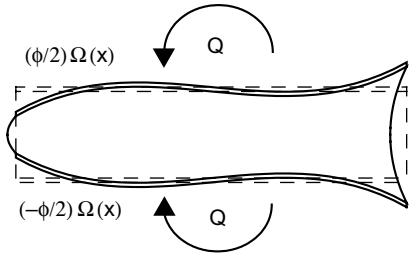

Fig. 4. Deformation under warping moment.

Under the combined loading of P, M and Q, the displacements of the elastomer in the x and z coordinate directions, denoted as u and w, respectively, are assumed to have the form

$$u(x,z) = u_0(x)\left(1 - \frac{4z^2}{t_e^2}\right) + u_1(x) \tag{2}$$

$$w(x,z) = (-\Delta - x\psi + \Omega\phi)\frac{z}{t_e} \tag{3}$$

In Eq. (2), the term of u_0 represents the kinematics assumption that vertical lines in the elastomer become parabolic after deformation; the horizontal deformation is supplemented by additional displacement u_1 that is constant through the thickness and is intended to accommodate the stretch of the reinforcement. Eq. (3) represents the assumption that the vertical deformation in the elastomer is linearly varied with the thickness.

The elastomer is assumed to be incompressible, which means that the summation of normal strain components is negligible and produces a constraint on displacements in the form

$$u_{,x} + w_{,z} = 0 \tag{4}$$

where the commas imply partial differentiation with respect to the indicated coordinate. Substituting Eqs. (2) and (3) into the above equation and then taking integration through the thickness from $z = -t_e/2$ to $z = t_e/2$ leads to

$$\frac{2}{3}u_{0,x} + u_{1,x} + \frac{1}{t_e}(-\Delta - x\psi + \Omega\phi) = 0 \tag{5}$$

The stress state in the elastomer is assumed to be dominated by the internal pressure p, such that the normal stress components of the elastomer, σ_{xx} and σ_{zz}, can be simplified as (Kelly, 1997)

$$\sigma_{xx} \approx \sigma_{zz} \approx -p \tag{6}$$

Under this stress assumption, the equilibrium equation in the x direction of the elastomer becomes

$$-p_{,x} + \tau_{xz,z} = 0 \tag{7}$$

where τ_{xz} is the shear stress having the form, from Eqs. (2) to (3),

$$\tau_{xz} = G_e\frac{z}{t_e}\left(-8\frac{u_0}{t_e} - \psi + \Omega_{,x}\phi\right) \tag{8}$$

with G_e being the shear modulus of the elastomer. Substitution of this into Eq. (7) gives

$$p_{,x} = \frac{G_e}{t_e}\left(-8\frac{u_0}{t_e} - \psi + \Omega_{,x}\phi\right) \tag{9}$$

The thickness of reinforcements is much smaller than the thickness of elastomeric layers, so that the deformation of reinforcements in the vertical direction can be neglected and only the deformation in the horizontal direction is considered. In the laminated elastomeric bearing, the top and bottom surfaces of the reinforcement are bonded to the layers of the elastomer. The internal forces acting in the reinforcing sheet are related to the shear stresses of the elastomeric layers through the equilibrium equation in the x direction (Tsai and Kelly, 2001)

$$N_{xx,x}(x) + \tau_{xz}(x, -t_e/2) - \tau_{xz}(x, t_e/2) = 0 \tag{10}$$

where N_{xx} is the normal force in the x direction acting in unit length of the reinforcement along the y direction. Substitute Eq. (8) into (10) and then combine the result with Eq. (9), which leads to

$$N_{xx,x} = t_e p_{,x} \tag{11}$$

At the edges of the pad, the normal stresses of the elastomer and the reinforcement are free, i.e. $p(a) = 0$ and $N_{xx}(a) = 0$, which indicates that, from Eq. (11),

$$N_{xx}(x) = t_e p(x) \tag{12}$$

The deformation in the reinforcement can be regarded as being in plane stress state within the x–y plane, such that the stress–strain relation of the reinforcement is

$$u_{1,x} = \frac{1 - v_f^2}{E_f t_f} N_{xx} \tag{13}$$

where E_f and v_f are the elastic modulus and Poisson's ratio of the reinforcement. Using Eqs. (12) and (13), Eq. (5) becomes

$$\frac{2}{3} u_{0,x} = -\frac{1 - v_f^2}{E_f t_f} t_e p - \frac{1}{t_e}(-\Delta - x\psi + \Omega\phi) \tag{14}$$

Differentiating Eq. (9) with respect to x and then using Eq. (14) to eliminate the term of $u_{0,x}$ leads to

$$p_{,xx} - \alpha^2 p = 12 \frac{G_e}{t_e^3}\left[-\Delta - x\psi + \left(\Omega + \frac{1}{12} t_e^2 \Omega_{,xx}\right)\phi\right] \tag{15}$$

in which α is defined as

$$\alpha = \sqrt{\frac{12 G_e (1 - v_f^2)}{E_f t_f t_e}} \tag{16}$$

The shape factor of the elastomeric layer in the infinitely long strip pad is defined as $S = a/t_e$. The term on the right-hand side of Eq. (15), $t_e^2 \Omega_{,xx}/12$, which is equal to $x/(2aS^2)$, is negligible because the "pressure approach" is applicable to isolators with shape factors greater than about five (Kelly, 1997). With the boundary condition $p(a) = 0$, the solution of the pressure in Eq. (15) has the form

$$p(x) = p_\Delta(x) + p_\psi(x) + p_\phi(x) \tag{17}$$

in which p_Δ is the pressure distribution in the elastomer under the compression force P,

$$p_\Delta(x) = \frac{12 G_e S^2}{(\alpha a)^2}\left(\frac{\Delta}{t_e}\right)\left(1 - \frac{\cosh \alpha x}{\cosh \alpha a}\right) \tag{18}$$

p_ψ is the pressure distribution in the elastomer under the bending moment M,

$$p_\psi(x) = \frac{12 G_e S^2}{(\alpha a)^2}\left(\frac{a\psi}{t_e}\right)\left(\frac{x}{a} - \frac{\sinh \alpha x}{\sinh \alpha a}\right) \tag{19}$$

and p_ϕ is the pressure distribution in the elastomer under the warping moment Q,

$$p_\phi(x) = -\frac{12 G_e S^2}{(\alpha a)^2}\left(\frac{\phi}{t_e}\right)\left\{\left(\frac{x}{a}\right)^3 + \left[\omega + \frac{6}{(\alpha a)^2}\right]\frac{x}{a} - \left[1 + \omega + \frac{6}{(\alpha a)^2}\right]\frac{\sinh \alpha x}{\sinh \alpha a}\right\} \tag{20}$$

3. Effective stiffness of reinforced layers

Under the combined loading of P, M and Q, the internal virtual work of a single layer of elastomer and a sheet of reinforcement is dominated by

$$\delta W_i = \int_{-t_e/2}^{t_e/2} \int_A \sigma_{zz}\delta\varepsilon_{zz}\,\mathrm{d}A\,\mathrm{d}z + \frac{E_f t_f^3}{12(1-\nu_f^2)} \int_{-a}^{a} w_{,xx}(x,t_e/2)\delta w_{,xx}(x,t_e/2)\,\mathrm{d}x \tag{21}$$

in which the second term of the right-hand side is the virtual work for the flexure deformation of the reinforcement, and the first term is the virtual work done by the normal stress in the elastomeric layer which can be expressed as

$$\int_{-t_e/2}^{t_e/2} \int_A \sigma_{zz}\delta\varepsilon_{zz}\,\mathrm{d}A\,\mathrm{d}z = \int_{-a}^{a} (p_\Delta + p_\psi + p_\phi)(\delta\Delta + x\delta\psi - \Omega\delta\phi)\,\mathrm{d}x \tag{22}$$

In order to allow the virtual work to be decoupled as

$$\int_{-t_e/2}^{t_e/2} \int_A \sigma_{zz}\delta\varepsilon_{zz}\,\mathrm{d}A\,\mathrm{d}z = \int_{-a}^{a} (p_\Delta\delta\Delta + p_\psi x\delta\psi - p_\phi\Omega\delta\phi)\,\mathrm{d}x \tag{23}$$

we need to select a warping function Ω such that

$$\int_{-a}^{a} p_\psi \Omega\,\mathrm{d}x = 0 \tag{24}$$

and

$$\int_{-a}^{a} p_\phi x\,\mathrm{d}x = 0 \tag{25}$$

Substitution of Eqs. (1) and (19) into Eq. (24) leads to

$$\int_{-a}^{a} \left(\frac{x}{a} - \frac{\sinh\alpha x}{\sinh\alpha a}\right)\left[\left(\frac{x}{a}\right)^3 + \omega\left(\frac{x}{a}\right)\right]\mathrm{d}x = 0 \tag{26}$$

from which ω is solved as

$$\omega = -\left[1 + \frac{6}{(\alpha a)^2} + \frac{\frac{2}{15}(\alpha a)^2}{\frac{\alpha a}{\tanh\alpha a} - 1 - \frac{1}{3}(\alpha a)^2}\right] \tag{27}$$

Substituting Eq. (20) into (25), we obtain the same form of ω as the above equation. Therefore, the warping function Ω with the warping coefficient in Eq. (27) satisfies the decoupled conditions in Eqs. (24) and (25).

Considering the compression force P only as shown in Fig. 2, the principle of virtual work gives

$$P\delta\Delta = t_e \int_{-a}^{a} (-p_\Delta)\delta\left(-\frac{\Delta}{t_e}\right)\mathrm{d}x \tag{28}$$

Substituting Eq. (18) into the above equation yields

$$P = (EA)_{\mathrm{eff}}\frac{\Delta}{t_e} \tag{29}$$

where $(EA)_{\mathrm{eff}}$ is the effective compression stiffness defined as

$$(EA)_{\mathrm{eff}} = aG_eS^2\frac{24}{(\alpha a)^2}\left(1 - \frac{\tanh\alpha a}{\alpha a}\right) \tag{30}$$

Considering the bending moment M only as shown in Fig. 3, the principle of virtual work gives

$$M\delta\psi = t_e \int_{-a}^{a} (-p_\psi)\delta\left(-x\frac{\psi}{t_e}\right)\mathrm{d}x \tag{31}$$

Substituting Eq. (19) into the above equation, the resultant moment becomes

$$M = (EI)_{\text{eff}}\frac{\psi}{t_e} \tag{32}$$

where $(EI)_{\text{eff}}$ is the effective bending stiffness defined as

$$(EI)_{\text{eff}} = a^3 G_e S^2 \frac{24}{(\alpha a)^4}\left[1 + \frac{1}{3}(\alpha a)^2 - \frac{\alpha a}{\tanh \alpha a}\right] \tag{33}$$

Considering the warping moment Q only as shown in Fig. 4, the principle of virtual work gives

$$Q\delta\phi = t_e \int_{-a}^{a} (-p_\phi)\delta\left(\Omega\frac{\phi}{t_e}\right)\mathrm{d}x + \frac{E_f t_f^3}{12(1-v_f^2)}\int_{-a}^{a} \Omega_{,xx}\frac{\phi}{2}\delta\left(\Omega_{,xx}\frac{\phi}{2}\right)\mathrm{d}x \tag{34}$$

Substituting Eqs. (1) and (20) into Eq. (34) and using the condition in Eq. (26) lead to

$$Q = (EJ)_{\text{eff}}\frac{\phi}{t_e} \tag{35}$$

where $(EJ)_{\text{eff}}$ is the effective warping stiffness defined as

$$(EJ)_{\text{eff}} = aG_e S^2\left[\frac{16}{5(\alpha a)^2}\left(-\frac{3}{7}-\omega\right) + \frac{1}{2\lambda S^3 (a/t_f)^3}\right] \tag{36}$$

with λ being

$$\lambda = \frac{(1-v_f^2)G_e}{E_f} \tag{37}$$

4. Shear deformation

Under the lateral shear force, the shear deformation in the elastomeric layer consists of two parts as shown in Fig. 5. One is related to the pure shear where the reinforcements remain planar and rotate an angle ψ; the slope of the lateral deformation is θ. The other is related the warping shear where the top and bottom reinforcements have the same warping deformation. The horizontal and vertical displacements corresponding to the shear deformation have the forms

$$u(x,z) = \theta z \tag{38}$$

$$w(x,z) = -x\psi + \Omega\phi \tag{39}$$

The internal virtual work of a single layer of elastomer and a sheet of reinforcement for the shear deformation is

$$\delta W_i = \int_{-t_e/2}^{t_e/2}\int_A \tau_{xz}\delta\gamma_{xz}\,\mathrm{d}A\,\mathrm{d}z + \frac{E_f t_f^3}{12(1-v_f^2)}\int_{-a}^{a} w_{,xx}(x,t_e/2)\delta w_{,xx}(x,t_e/2)\,\mathrm{d}x \tag{40}$$

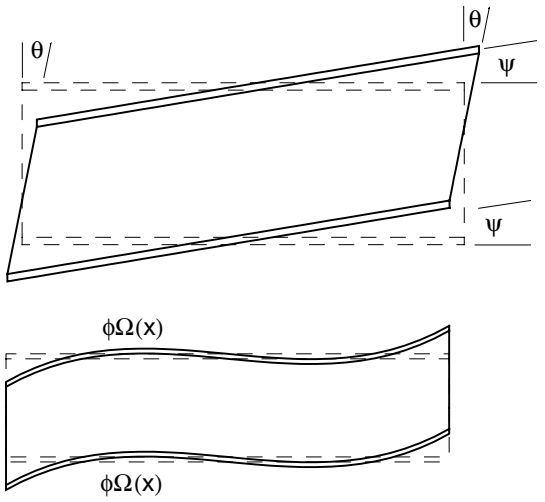

Fig. 5. Deformation under shear force and warping shear.

in which the second term of the right-hand side is the virtual work for the flexure deformation of the reinforcement. Substituting Eqs. (38) and (39) into the above equation leads to

$$\delta W_i = \left[t_e G_e \int_{-a}^{a} (\theta - \psi + \Omega_{,x}\phi)\,\mathrm{d}x\right]\delta(\theta - \psi) + \left[t_e G_e \int_{-a}^{a} (\theta - \psi + \Omega_{,x}\phi)\Omega_{,x}\,\mathrm{d}x + \frac{2E_f t_f^3}{(1 - \nu_f^2)a^3}\phi\right]\delta\phi \tag{41}$$

which can be expressed in terms of force resultants as

$$\delta W_i = V t_e \delta(\theta - \psi) + R t_e \delta\phi \tag{42}$$

where V is the shear force and R is the warping shear. From Eqs. (41) and (42), we have

$$V = G_e A(\theta - \psi) + G_e B\phi \tag{43}$$

$$R = G_e B(\theta - \psi) + G_e C\phi \tag{44}$$

in which $A = 2a$ is the area of an unit length of the elastomeric layer; B and C are the two cross-section properties of warping defined as

$$B = \int_{-a}^{a} \Omega_{,x}\,\mathrm{d}x = 2(1 + \omega) \tag{45}$$

$$C = \int_{-a}^{a} \Omega_{,x}^2\,\mathrm{d}x + \frac{2E_f t_f^3}{t_e G_e (1 - \nu_f^2)a^3} = \frac{2}{a}\left[\frac{4}{5} + (1 + \omega)^2 + \frac{S}{\lambda(a/t_f)^3}\right] \tag{46}$$

where λ has been defined in Eq. (37).

The theory of Tsai and Kelly (in press) uses the two warping-related normal forces, N_B and N_C. In the reinforced elastomeric layer, these normal forces are defined as

$$N_B = \int_{-a}^{a} p_\Delta \Omega_{,x}\,\mathrm{d}x \tag{47}$$

$$N_C = \int_{-a}^{a} p_\Delta \Omega_{,x}^2\,\mathrm{d}x \tag{48}$$

Using Eqs. (18) and (29), the above equations become

$$N_B = f_B \frac{P}{A} \tag{49}$$

$$N_C = f_C \frac{P}{A} \tag{50}$$

with

$$f_B = 2\left[1 + \omega + \frac{6}{(\alpha a)^2} - \frac{2}{\left(\frac{\alpha a}{\tanh \alpha a} - 1\right)}\right] \tag{51}$$

$$f_C = \frac{8}{a}\left\{\frac{1}{5} + \frac{6}{(\alpha a)^2} + \frac{45}{(\alpha a)^4} + \frac{1}{4}\left[1 + \omega + \frac{6}{(\alpha a)^2}\right]^2 - \left[\frac{\frac{9}{5} + \omega + \frac{18}{(\alpha a)^2}}{\frac{\alpha a}{\tanh \alpha a} - 1}\right]\right\} \tag{52}$$

5. Stiffness equivalent to homogeneous beam

To apply the beam theory of Tsai and Kelly to analyze the multilayer isolators, the stiffness of a single reinforced layer of elastomer derived in the previous sections has to convert to the stiffness of an equivalent homogeneous beam. For the homogeneous beam, the bending stiffness and warping stiffness are defined as

$$M = EI\psi_{,z} \quad \text{and} \quad Q = EJ\phi_{,z} \tag{53}$$

However, the bending stiffness and warping stiffness of the single reinforced layer, presented in Eqs. (32) and (35), are

$$M = (EI)_{\text{eff}} \frac{\psi}{t_e} \quad \text{and} \quad Q = (EJ)_{\text{eff}} \frac{\phi}{t_e} \tag{54}$$

in which ψ and ϕ are constant through the thickness of the elastomeric layer. If there are n layers of the elastomer in the isolator, we have the following equivalence

$$\psi_{,z} = \frac{n\psi}{h} \quad \text{and} \quad \phi_{,z} = \frac{n\phi}{h} \tag{55}$$

in which h is the height of the isolator. The bending stiffness and warping stiffness of the equivalent homogeneous beam become

$$EI = (EI)_{\text{eff}} \frac{h}{nt_e} \quad \text{and} \quad EJ = (EJ)_{\text{eff}} \frac{h}{nt_e} \tag{56}$$

Similarly, the shear modulus for the equivalent homogeneous beam is

$$G = G_e \frac{h}{nt_e} \tag{57}$$

According to the theory of Tsai and Kelly (in press), when a vertical compression force and a horizontal lateral force act on one end of the isolator, the lateral stiffness of the isolator K_H can be expressed in terms of the normalized compression force $P/(GA)$, the rigidity ratio of the elastomer ρ defined as

$$\rho = \frac{EI}{GAh^2} = \frac{(EI)_{\text{eff}}}{G_e A h^2} \tag{58}$$

and the two warping parameters κ_b and κ_c defined as

$$\kappa_b = \frac{EI}{EJ}\left(\frac{GB+N_B}{GA}\right)^2 = \frac{(EI)_{\text{eff}}}{(EJ)_{\text{eff}}}\left(\frac{B}{A}+\frac{f_B}{A}\frac{P}{GA}\right)^2 \tag{59}$$

$$\kappa_c = \frac{EI}{EJ}\left(\frac{GC+N_C}{GA}\right) = \frac{(EI)_{\text{eff}}}{(EJ)_{\text{eff}}}\left(\frac{C}{A}+\frac{f_C}{A}\frac{P}{GA}\right) \tag{60}$$

The cross-sectional properties, $(EI)_{\text{eff}}$ in Eq. (33), $(EJ)_{\text{eff}}$ in Eq. (36), B in Eq. (45), C in Eq. (46), f_B in Eq. (51), and f_C in Eq. (52), are the functions of αa which is a parameter of the extension rigidity of the reinforcement. From Eqs. (16) and (37), we know

$$\alpha a = \sqrt{12\lambda S\frac{a}{t_f}} \tag{61}$$

When the reinforcement becomes inextensible, $\alpha a \to 0$. Usually, αa is a small number, such that its high-order terms can be neglected. Substituting the following series expansion

$$\frac{\alpha a}{\tanh \alpha a} \approx 1+\frac{1}{3}(\alpha a)^2-\frac{1}{45}(\alpha a)^4+\frac{2}{945}(\alpha a)^6-\frac{1}{4725}(\alpha a)^8+\frac{2}{93555}(\alpha a)^{10} \tag{62}$$

into Eq. (27) and neglecting the high-order terms of αa, the warping coefficient becomes

$$\omega \approx -\frac{3}{7}\left[1+\frac{2}{315}(\alpha a)^2\right] \tag{63}$$

Using Eqs. (62) and (63) and neglecting the high-order terms of αa, the cross-sectional properties can be reduced to

$$(EI)_{\text{eff}} \approx a^3 G_e S^2 \frac{8}{15}\left[1-\frac{2}{21}(\alpha a)^2\right] \tag{64}$$

$$(EJ)_{\text{eff}} \approx aG_eS^2\left\{\frac{32}{3675}\left[1-\frac{2}{77}(\alpha a)^2\right]+\frac{1}{2\lambda S^3(a/t_f)^3}\right\} \tag{65}$$

$$B \approx \frac{8}{7}\left[1-\frac{1}{210}(\alpha a)^2\right] \tag{66}$$

$$C \approx \frac{1}{a}\left\{\frac{552}{245}\left[1-\frac{4}{1449}(\alpha a)^2\right]+\frac{2S}{\lambda(a/t_f)^3}\right\} \tag{67}$$

$$f_B \approx \frac{12}{35}\left[1+\frac{16}{315}(\alpha a)^2\right] \tag{68}$$

$$f_C \approx \frac{1}{a}\frac{216}{245}\left[1+\frac{26}{945}(\alpha a)^2\right] \tag{69}$$

Substituting Eq. (64) into (58) and using $A = 2a$ gives

$$\rho \approx \frac{4}{15}S^2\left(\frac{a}{h}\right)^2\left[1-\frac{2}{21}(\alpha a)^2\right] \tag{70}$$

Substituting Eqs. (64)–(69) into Eqs. (59) and (60) gives

$$\kappa_b \approx \frac{20\left[1-\frac{2}{21}(\alpha a)^2\right]\left\{1-\frac{1}{210}(\alpha a)^2+\left[\frac{3}{10}+\frac{8}{525}(\alpha a)^2\right]\frac{P}{GA}\right\}^2}{\left[1-\frac{2}{77}(\alpha a)^2+\frac{3675}{64\lambda S^3(a/t_f)^3}\right]} \tag{71}$$

$$\kappa_c \approx \frac{3\left[1-\frac{2}{21}(\alpha a)^2\right]\left\{23-\frac{4}{63}(\alpha a)^2+\left[9+\frac{26}{105}(\alpha a)^2\right]\frac{P}{GA}+\frac{245S}{12\lambda(a/t_f)^3}\right\}}{\left[1-\frac{2}{77}(\alpha a)^2+\frac{3675}{64\lambda S^3(a/t_f)^3}\right]} \tag{72}$$

6. Lateral stiffness and buckling load of isolators

Based on the theory of Tsai and Kelly (in press), Eqs. (70)–(72) indicates that the dimensionless lateral stiffness of isolators $K_H h/(GA)$ is a function of the normalized compression force $P/(GA)$, the modulus ratio of the elastomer to the reinforcement λ, the shape factor of the elastomer S, the width-thickness ratio of the reinforcement a/t_f and the width-height ratio of the isolator a/h. For the isolator with $G_e = 0.7\,\text{MPa}$, $E_f = 0.21\times10^6\,\text{MPa}$ and $\nu_f = 0.3$, the corresponding λ value in Eq. (37) is $\lambda = 3\times10^{-6}$. For this particular λ value, the lateral stiffness calculated from the theory of Tsai and Kelly is plotted as a function of compression force in Fig. 6 for $S = 10$, $a/h = 1$ and different a/t_f values, in Fig. 7 for $S = 10$, $a/t_f = 80$ and different a/h values, and in Fig. 8 for $a/t_f = 80$, $a/h = 1$ and different S values. These figures show that the lateral stiffness decreases with increasing the compression force. Larger reinforcement thickness, smaller bearing height or larger shape factor of the elastomer will have higher lateral stiffness.

The buckling occurs when the lateral stiffness $K_H = 0$. Based on the theory of Tsai and Kelly, the equation of buckling load P_{cr} becomes

$$\begin{aligned}
&\frac{(EI)_{\text{eff}}}{(EJ)_{\text{eff}}}\left[\frac{f_C}{A}-\left(\frac{f_B}{A}\right)^2\right]\left(\frac{P_{cr}}{GA}\right)^3+\left\{\frac{(EI)_{\text{eff}}}{(EJ)_{\text{eff}}}\left(\frac{C}{A}+\frac{f_C}{A}-2\frac{f_B B}{A^2}\right)+\pi^2\rho\left[1+\frac{(EI)_{\text{eff}}}{(EJ)_{\text{eff}}}\left(\frac{f_B}{A}\right)^2\right]\right\}\left(\frac{P_{cr}}{GA}\right)^2\\
&\quad+\left\{\frac{(EI)_{\text{eff}}}{(EJ)_{\text{eff}}}\left[\frac{C}{A}-\left(\frac{B}{A}\right)^2\right]+\pi^2\rho\left[1+\frac{(EI)_{\text{eff}}}{(EJ)_{\text{eff}}}\left(2\frac{f_B B}{A^2}-\frac{f_C}{A}\right)\right]\right\}\left(\frac{P_{cr}}{GA}\right)\\
&\quad-\left\{\pi^2\rho\frac{(EI)_{\text{eff}}}{(EJ)_{\text{eff}}}\left[\frac{C}{A}-\left(\frac{B}{A}\right)^2\right]+\pi^4\rho^2\right\}\\
&\quad=0
\end{aligned} \tag{73}$$

This is a cubic equation of the buckling load and can be solved by the numerical method for the specified values of λ, S, a/t_f and a/h. For the isolators of $\lambda = 3\times10^{-6}$, the variation of the buckling load with a/h is plotted in Figs. 9 and 10 for $S = 10$ and 20, respectively, which compare the buckling loads of different reinforcement thicknesses and rigid reinforcement. The buckling load for the rigid reinforcement has the form (Kelly, 1997; Tsai and Kelly, in press)

$$(P_{cr})_{\text{rigid}} = GA\left(\frac{-1+\sqrt{1+4\pi^2\rho}}{2}\right) \tag{74}$$

These figures show that the buckling load almost linearly varies with a/h and has little change between $a/t_f = 160$ and 320.

The ratios of P_{cr} solved from Eq. (73) to $(P_{cr})_{\text{rigid}}$ shown in Eq. (74) are plotted as a function of reinforcement thickness in Figs. 11 and 12 for $S = 10$ and 20, respectively, which show that the buckling load

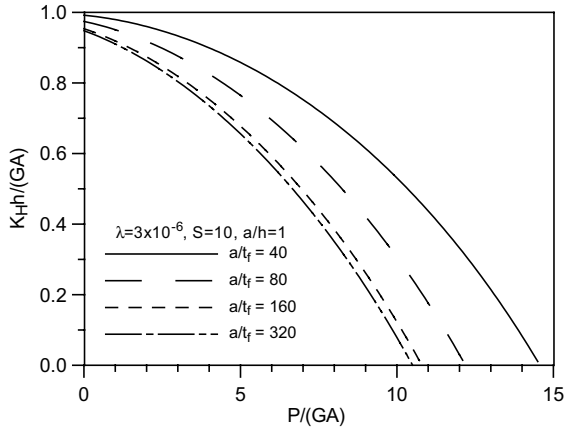

Fig. 6. Lateral stiffness as a function of compression load for different values of a/t_f.

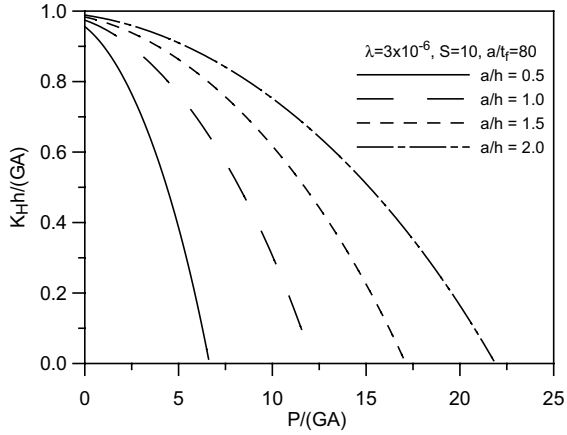

Fig. 7. Lateral stiffness as a function of compression load for different values of a/h.

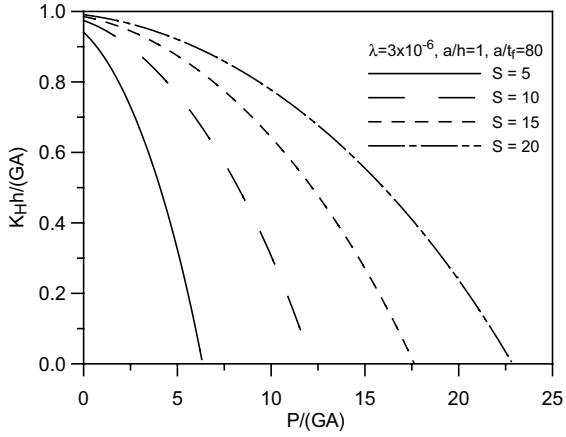

Fig. 8. Lateral stiffness as a function of compression load for different values of S.

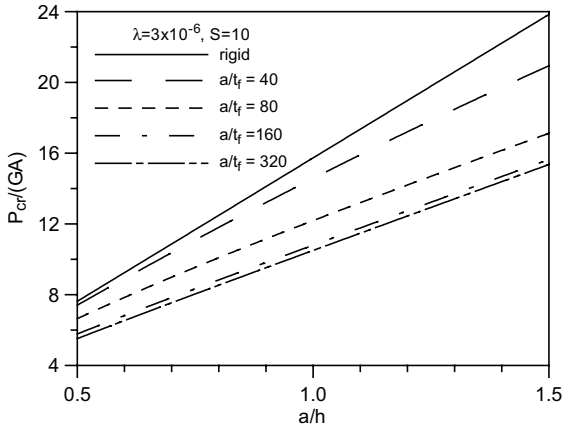

Fig. 9. Buckling load varied with bearing height for $S = 10$.

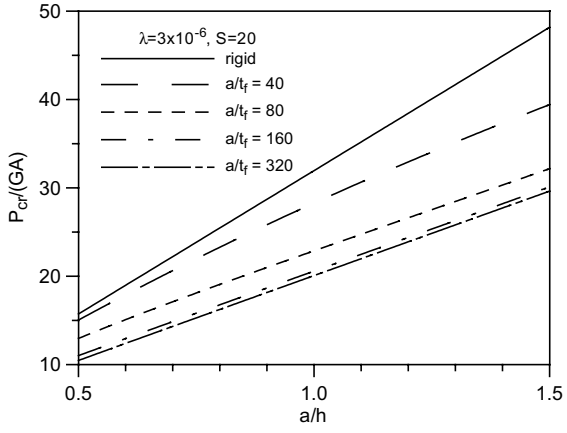

Fig. 10. Buckling load varied with bearing height for $S = 20$.

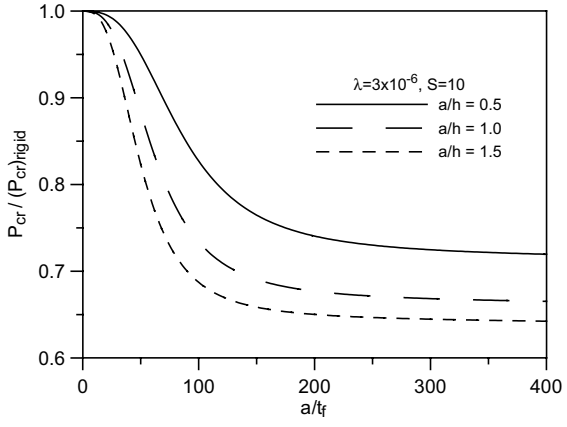

Fig. 11. Buckling load varied with reinforcement thickness for $S = 10$.

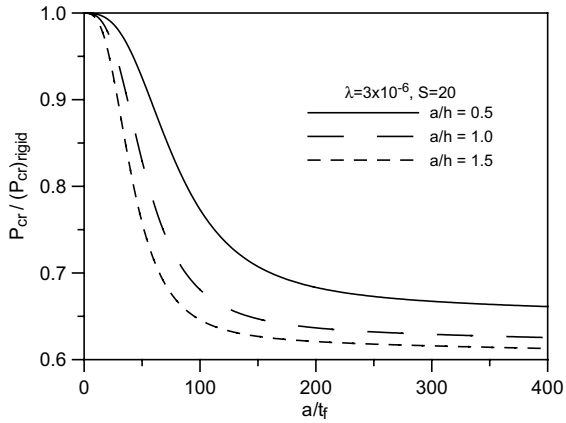

Fig. 12. Buckling load varied with reinforcement thickness for $S = 20$.

decreases with reducing the reinforcement thickness. After the thickness is reduced to about $a/t_f = 150$, there is only a negligible further reduction in the buckling load.

7. Conclusion

An analysis has been developed for the buckling load of elastomeric multilayer isolators that includes the effect of the flexibility of the steel reinforcing plates. This analysis has treated the isolator as a short elastic column in which shear deformation and warping of the cross-section are included. Pressure distributions in the elastomeric layer bonded to flexible reinforcements under compression force, bending moment and warping moment are derived from an assumed displacement field. The warping function of the cross-section is determined from the condition that the compression force and bending moment are independent of the warping function. After the warping-related parameters are established, the lateral stiffness of the isolator varied with the compression load can be solved by the beam theory, from which a cubic equation for the buckling load of the isolators is derived.

The buckling load of the isolators is a function of the ratio of elastic modulus between the elastomeric layer and the reinforcement, the shape factor of the elastomeric layer, the width-thickness ratio of the reinforcement and the width-height ratio of the isolator. The buckling load decreases with reducing the reinforcement thickness. After the width-thickness ratio of the reinforcement is larger than 150, there is only a negligible further reduction in the buckling load. The flexibility effect of reinforcements on the buckling load of isolators is studied through the beam theory that assumes the warping of the cross-section is a cubic function. To justify the accuracy of using this beam theory to study seismic isolators, further study by comparing the theoretical results with the numerical solutions of finite element analysis or the experimental test of real models is required.

References

Gent, A.N., 1964. Elastic stability of rubber compression spring. Journal of Mechanical Engineering Science 6, 318–326.

Gent, A.N., Lindley, P.B., 1959. The compression of bonded rubber block. Proceeding of the Institution Mechanical Engineers 173, 111–117.

Gent, A.N., Meinecke, E.A., 1970. Compression, bending and shear of bonded rubber blocks. Polymer Engineering and Science 10, 48–53.

Haringx, J.A., 1948. On highly compressible helical spring and rubber rods, and their application for vibration-free mountings—part III. Philips Research Report 4, 206–220.

Kelly, J.M., 1994. The influence of plate flexibility on the buckling load of elastomeric isolators. Report UCB/EERC-94/03, Earthquake Engineering Research Center, University of California, Berkeley.

Kelly, J.M., 1997. Earthquake-Resistant Design with Rubber, second ed. Springer-Verlag, London.

Tsai, H.-C., Hsueh, S.-J., 2001. Mechanical properties of isolation bearings identified by a viscoelastic model. International Journal of Solid and Structures 38, 53–74.

Tsai, H.-C., Kelly, J.M., 2001. Stiffness analysis of fiber-reinforced elastomeric isolators. PEER Report No. 2001/05, Pacific Earthquake Engineering Research Center, University of California, Berkeley.

Tsai, H.-C., Kelly, J.M., 2002a. Stiffness analysis of fiber-reinforced rectangular seismic isolators. Journal of Engineering Mechanics, ASCE 128, 462–470.

Tsai, H.-C., Kelly, J.M., 2002b. Bending stiffness of fiber-reinforced circular seismic isolators. Journal of Engineering Mechanics, ASCE 128, 1150–1157.

Tsai, H.-C., Kelly, J.M. (in press). Buckling of short beams with warping effect included. International Journal of Solid and Structures. In this issue.

Tsai, H.-C., Lee, C.-C., 1998. Compressive stiffness of elastic layers bonded between rigid plates. International Journal of Solid and Structures 35, 3053–3069.

Tsai, H.-C., Lee, C.-C., 1999. Tilting stiffness of elastic layers bonded between rigid plates. International Journal of Solid and Structures 36, 2485–2505.